Reaction Kinetics, Mechanisms and Catalysis (2023) 136:727–740
https://doi.org/10.1007/s11144-023-02373-4

Catalytic dehydration of 2-propanol over nickel phosphide immobilized on natural bentonite

Hasanudin Hasanudin[1,2] · Wan Ryan Asri[1,2] · Lepa Husnia[1,2] · Zainal Fanani[1,2] · Roni Maryana[3] · Muhammad Al Muttaqii[3] · Zongyuan Zhu[4] · Suresh Sagadevan[5]

Received: 7 January 2023 / Accepted: 14 February 2023 / Published online: 22 February 2023

Abstract

This study investigated the fabrication of nickel phosphide immobilized on natural bentonite (NiP/bentonite) as a low-cost catalyst with different metal loadings (mEq/g) to produce diisopropyl ether (DIPE) as a potential gasoline additive. The catalysts were prepared using a simple wet-impregnation method. The physicochemical features of the parent natural bentonite and NiP/bentonite were analyzed using FTIR, SEM–EDX, XRD, N_2 physisorption, and catalyst acidity using the NH_3 gravimetric method. The dehydration reaction was conducted under mild conditions (150 °C for 3 h) using a reflux system. The results suggested that the NiP species did not alter the bentonite structure while increasing its acidity and surface area properties. Using the 8 mEq/g NiP/bentonite catalyst, a DIPE product of 68.52% was achieved owing to the highly acidic sites of the catalyst and high stability over three cycles. This study highlights the potential of nickel-phosphide-supported natural bentonite in the dehydration reaction for DIPE production.

Keywords Diisopropyl ether · 2-propanol dehydration · Nickel phosphide · Natural bentonite

✉ Hasanudin Hasanudin
hasanudin@mipa.unsri.ac.id

[1] Department of Chemistry, Faculty of Mathematics and Natural Science, Universitas Sriwijaya, Indralaya 30662, Indonesia

[2] Biofuel Research Group, Laboratory of Physical Chemistry, Faculty of Mathematics and Natural Science, Universitas Sriwijaya, Indralaya 30662, Indonesia

[3] Research Center for Chemistry, Indonesian Institute of Sciences, Building 452 Kawasan PUSPIPTEK, Serpong, Tangerang Selatan, Banten, Indonesia

[4] School of Energy and Power, Jiangsu University of Science and Technology, Zhenjiang 212000, China

[5] Nanotechnology & Catalysis Research Centre, Universiti Malaya, 50603 Kuala Lumpur, Malaysia

Introduction

Natural bentonite is the most frequently discovered mineral in Asia, particularly in Indonesia. This mineral is a silicate crystal with a layered structure [1]. Natural bentonite can expand and has a high ion exchange capacity, allowing it to absorb large amounts of interlayer cations [2]. This material has been extensively employed in many applications such as biolubricants [3], dye removal [4], hydrocracking catalysts [5, 6], phosphate removal [7], and Cr removal [8]. Under these conditions, the workability of bentonite is insufficient [9]. Because the properties of natural bentonite can be tuned, it is imperative to make modifications to enhance its performance and thus obtain a better product that inherently promotes its utilization for many potential applications [10]. The bentonite modification technique aims to improve the physicochemical features. The development of bentonite-based materials as catalysts and supported catalysts has proliferated because they are inexpensive and readily abundant [11]. In the context of the catalyst, textural and acidity features crucially affect the catalytic activity. One fabrication approach can be established by dispersing or incorporating the active species into the pore and/or the surface bentonite [12].

Presently, various species such as Fe, Ti, Zr, Al [12], Sn, Cr, LDH-based on polyoxo-vanadate and molybdate [13], Al/Fe [14], Zr [15], Co [16], Zr–Al [11], and Fe–Cr [17], have been explored and combined with bentonite. Recently, transition metal phosphide-based catalysts have been explored because of their high catalytic activity and selectivity for hydrogen and oxygen evolution reactions [18]. These materials are phosphorus transition metal compounds that combine the physical features of ceramics, including hardness and strength, with the electrical properties of metals, such as conductivity. Transition metal phosphides have been proposed as favorable catalysts owing to their low cost, abundance, and high efficiency [19]. The metal and P sites on the catalyst surface behave as proton acceptors and hydride receptor centers and are capable of replacing noble metal catalysts such as Pt [20]. The presence of phosphorus, which exerts a "ligand" (or electronic) effect and is geometrically situated at the location of the metal, has been attributed to the outstanding performance of transition metal phosphides [21]. A series of Ni_2P, WP, Fe_2P, CoP, and MoP have been fabricated and employed for the hydrodesulfurization of fuel [22]. Metal phosphide-based catalysts have also been utilized in hydrodeoxygenation reactions [19–21, 23–26].

Among the transition metal phosphide catalysts, nickel phosphide catalysts have been extensively reported to have high surface areas and high catalytic activities for many applications, such as HDS, dehydrogenation, hydrodeoxygenation, electrocatalytic water splitting, and methane dry reforming [27–29]. de Souza et al. [20] have developed the NiP species supported on SiO_2, Al_2O_3, CeO_2, TiO_2, and $CeZrO_2$. Ruangudomsakul et al. [26] reported that the Ni_xP_y catalyst provided a high green diesel yield in the dehydrogenation of palm oil compared with CoP and CuP. Gonçalves et al. [21] revealed that the Ni_2P-supported ZrO_2 has higher HDO activity than Ni_2P/SiO_2. Wagner et al. [30] developed NiP-supported zeolite Y for quinoline hydrodenitrogenation.

To the best of our knowledge, no research has been done on the preparation of nickel phosphide-supported natural bentonite. The combination of these species provides a positive effect with a highly acidic active site and surface area, as well as a low-cost catalyst. Therefore, in the present study, a nickel phosphide-supported catalyst was used as a model for the dehydration of 2-propanol to diisopropyl ether. Diisopropyl ether (DIPE), as reported in the literature, has the potential to be used as a gasoline additive with the potential to reduce GHG emissions and other GHG emissions [31]. DIPE has good features that can increase the octane number of gasoline fuel and is environmentally friendly [32], compared with other chemicals such as MTBE, ETBE, and TAME [33]. In this regard, various catalysts have been utilized for 2-propanol dehydration [34–39], but nickel phosphide-supported natural bentonite has not been comprehensively discussed. The DIPE product was evaluated using nickel phosphide-supported bentonite and parent natural bentonite. The physicochemical features of the catalyst will be assessed using a series of analyses, such as XRD, FTIR, SEM–EDS, N_2 adsorption–desorption, and total acidity by the gravimetric method. The dehydration product will be investigated using GC–MS.

Experimental

Preparation of nickel phosphide immobilized on bentonite catalysts

In a typical preparation, natural bentonite (200-mesh) from Bayan was first saturated with NaCl solution (≥ 99.5% purity, Merck), as reported in a previous study [9]. The as-prepared Na-bentonite (5 g) was subsequently dispersed in a 0.1 M $NiCl_2{\cdot}6H_2O$ solution (≥ 98.0% purity, Merck) with various volumes and stirred for 1 h at room temperature. Afterward, 0.5 M $(NH_4)_2HPO_4$ solution (≥ 99.0% purity, Merck) was gradually dripped onto the solution until it reached a predetermined volume corresponding to nickel phosphate loadings of 2, 4, 6, and 8 mEq/g of catalyst. The solution was stirred at room temperature, and the temperature was gradually increased until a paste was formed. The paste was dried at 80 °C for 1 day and calcined at 350 °C for 30 min. The as-synthesized nickel phosphate-bentonite (~ 5 g) was dissolved in 50 mL of DW and reduced using a certain amount of $NaBH_4$ powder (≥ 96.0%, Merck) under a sonicator for 30 min. The powder was separated and dried at 80 °C for 1 day. The 200-mesh dried nickel phosphide-supported bentonite is denoted as NiP/bentonite.

Characterization of catalyst

The phases and crystal structures of Na-bentonite and NiP/bentonite were characterized using a Rigaku Mini Flex 600 Powder Diffractometer. The 2θ range of measurements from 5° to 80° with a step size of 0.0200° and a count time of 0.24 s. Shimadzu FTIR 8201 (KBr pellet method) was used to analyze the functional groups of both catalysts, with range of measurements from 4000 to 450 cm^{-1}. SEM micrographs of the catalysts were obtained using an SEM JSM 650, and the

elemental composition was determined using EDS. The textural properties of the catalysts were evaluated using Quantachrome NOVA. Prior to analysis, the catalyst was vacuum degassed up to 300 °C for 1 h with a heating rate of 10 °C/min. The surface areas of the catalysts were calculated using a multipoint BET procedure. The total acidity of the catalysts was determined gravimetrically using NH_3 as the probe. Before adsorption, the desiccator was vacuumed, saturated, and flowed with NH_3 vapor from the NH_4OH solution for 1 day (≥ 25.0% purity, Merck). The as-adsorbed NH_3 catalyst samples were quantitatively weighed, and the NH_3 absorbed catalyst (mmol NH_3/g catalyst) was calculated according to a previous study [9].

Catalytic activity test

In the catalytic activity test, 50 mL of 2-propanol (≥ 99.8% purity, Merck) was introduced into the boiling flask, followed by 0.5 g catalysts under the batch reactor. The dehydration was conducted at 150 °C for 210 min. The catalyst was then separated, and the product was analyzed using a Thermo Scientific GC–MS instrument. To investigate the reusability of the catalyst, the spent catalyst in the first cycle was washed several times with acetone, dried overnight at 120 °C, and used for the next cycle.

Results and discussion

Physicochemical characterization

The crystal structure and phases of the as-synthesized Na-bentonite and NiP/bentonite were assessed using XRD, as shown in Fig. 1. As shown in Fig. 1a, a

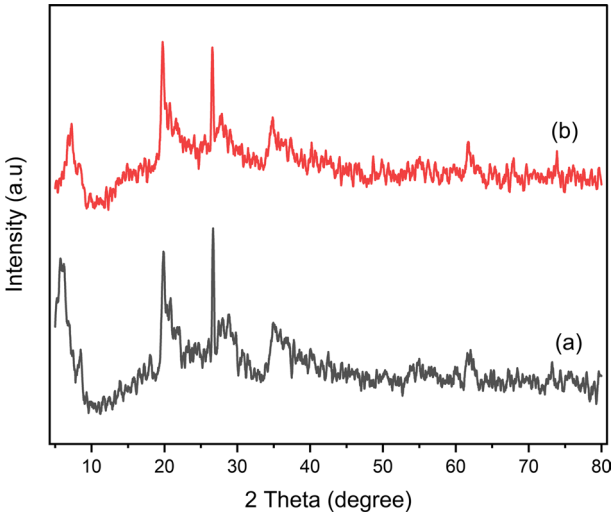

Fig. 1 XRD pattern (a) Na-bentonite and (b) NiP/bentonite

characteristic of the montmorillonite phase was observed at 2θ = 6.78°, 21.21°, 35.23°, and 62° [40]. Quartz phase impurities were also observed at 2θ = 26.43° and 29.23° [41]. These typical bentonite peaks have been consistently reported in other studies [42–44]. A typical nickel phosphide phase, as in other reports [22, 26, 45], is likely unobserved in the NiP/bentonite diffractogram (Fig. 1b), which suggests that this phase is amorphous [20]. This condition was also reported by González-castaño et al. [27], who reported that a highly crystalline phase of nickel phosphide could be achieved during high-temperature calcination. No appreciable change in the diffractogram of Na-bentonite after loading with nickel phosphide indicated that the main structure of bentonite was favorably maintained [21].

The IR bands characteristic of functional groups of parent Na-bentonite and NiP/bentonite are shown in Fig. 2. The absorption band at 3582 cm^{-1} (Fig. 2a) was related to the stretching vibration of the metal-OH in the octahedral layer of bentonite [46], whereas the adsorbed OH groups or water molecules can be found at 1625 cm^{-1} [4, 47]. The absorption band at 1035 cm^{-1} was assigned to the stretching vibration of the Si–O–Si bonds, and the absorption band at 922 cm^{-1} was attributed to the Al–OH vibration [48]. Al–O, Si–O, and Al–O–Si coexisted vibrations were observed at ca. 692 cm^{-1}, 432 cm^{-1}, and 761 cm^{-1}, respectively [49]. The FTIR spectrum of NiP/bentonite exhibited a distinct absorption band at 1350 cm^{-1}, which was attributed to the vibration of phosphate groups from NiP species [50–53]. NiP/bentonite displayed absorption bands similar to those of the parent bentonite, which is consistent with the XRD results.

SEM micrographs of both catalysts are presented in Fig. 3. Na-bentonite has sizeable aggregations of irregularly distributed platelets [54]. These platelets have a lamellar structure with sharp edges [55, 56] No appreciable surface morphological changes were observed in the SEM micrograph of NiP/bentonite (Fig. 3b).

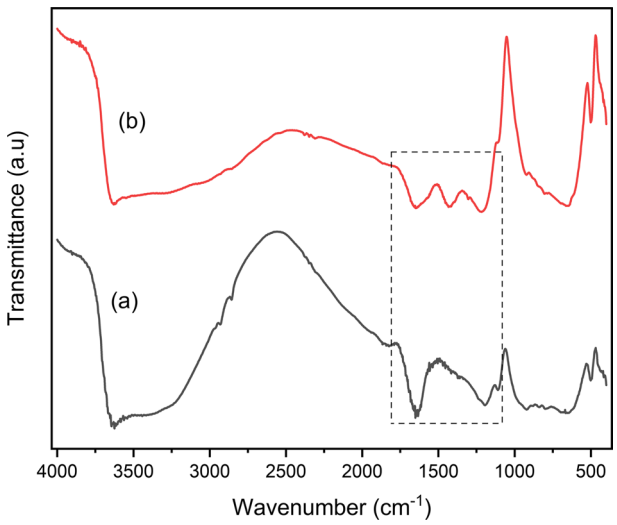

Fig. 2 FTIR spectra (a) Na-bentonite and (b) NiP/bentonite

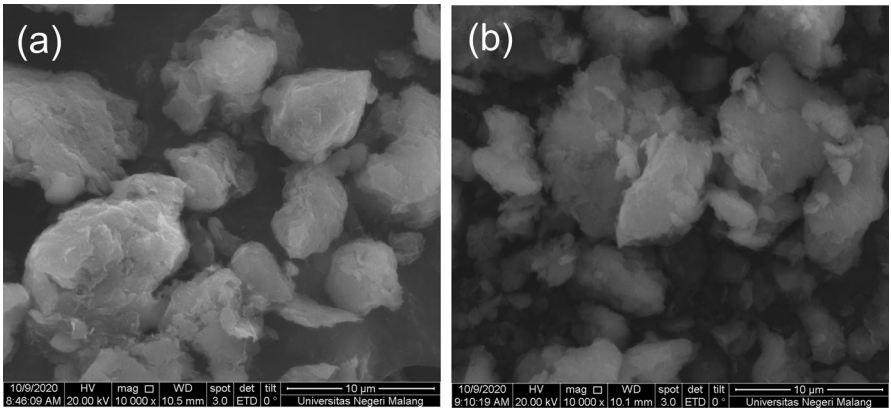

Fig. 3 SEM micrographs **a** Na-bentonite and **b** NiP/bentonite

A similar finding was reported by Pajarito et al. [48], who revealed no significant change in the surface morphology of Zn-bentonite compared with that of the parent bentonite.

EDS analysis (Table 1) showed that the Si/Al ratio was relatively unchanged, which suggested that the NiP species loaded towards the bentonite surface did not alter the main frameworks of bentonite [5], which is consistent with the XRD and FTIR results. Furthermore, P (1.66 wt.%) and Ni (3.23 wt.%) elements co-existed in the NiP/bentonite, which suggested that the NiP/bentonite catalyst was successfully prepared. Table 1 shows that Na-bentonite consists of various elements, as has been consistently reported in other studies [54]. The pre-existing P elements before Na-bentonite modification were possible because they originated from nature, although the content of the P element increased after modification. Abdou et al. [57] reported a similar finding when preparing Egyptian bentonite

Table 1 Elemental analysis of catalysts using EDS

Element	Atomic (wt.%)	
	Na-bentonite	NiP/bentonite
C	14.42	24.25
O	47.25	42.82
Na	2.02	2.25
Mg	2.42	2.08
Al	8.4	5.62
Si	20.8	13.92
Ca	0.45	0.37
Fe	3.51	2.78
Cl	0.61	0.73
P	0.12	1.66
Ni	0	3.23

($P_2O_5 = 0.16\%$). The EDS results suggest that the NiP species were capable of supporting bentonite without changing its main framework.

The N_2 adsorption–desorption curves of all catalysts are shown in Fig. 4. It can be seen that all catalysts had a type IV isotherm based on IUPAC categorization, which mainly indicated that the catalysts were mesoporous [58, 59]. de Oliveira et al. [55] stated that the disjunction of the adsorption–desorption curve at a relative pressure (ca. 0.4) is attributed to the appearance of small mesopores on the adsorbate. Monolayer nitrogen adsorption on the mesoporous wall occurred when P/Po was below 0.4, and capillary condensation occurred in mesopores with P/Po in the range of 0.4–0.8, which was revealed by a sharp increase and hysteresis in the adsorption isotherm. Multilayer adsorption can be observed on the outer surface of the particles at higher P/Po [58]. The hysteresis in Fig. 4 is recognized as type H4, which suggests a slit-shaped porous solid [14]. A previous study reported similar observations for other clay-based materials [3].

The textural features of the catalysts are presented in Table 2. It can be seen that the as-prepared NiP/bentonite surface area, diameter, and volume of pores were much higher than those of Na-bentonite. The surface area of catalysts increased as the metal loading increased. The increase in the corresponding textural features suggests that impregnation with NiP species promoted an increase in porosity and surface area. The increase in the BET surface areas of pillared natural bentonite samples may be attributed to the increase in pore volume and enlarged total pore volume owing to the presence of NiP species [60]. Another study also reported the same trend [61, 62]. Compared with a previous study [9], NiP/bentonite had a higher surface area than MoP-bentonite (63.69 m^2/g), which promoted more reactant to be adsorbed on the surface and affected the dehydration process over the catalyst's active site. However, prolonged metal loading (10 mEq/g) decreased the surface area of the catalyst as well as the pore diameter,

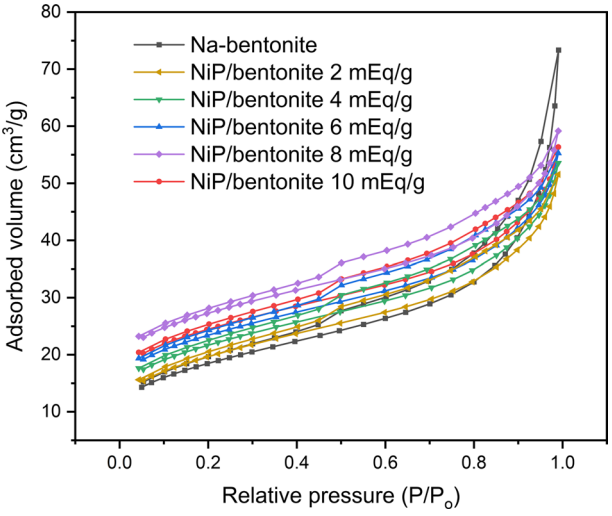

Fig. 4 N_2 adsorption–desorption isotherms of (a) Na-bentonite and (b) NiP/bentonite

Table 2 Textural features of Na-bentonite and NiP/bentonite

Catalyst	Surface area (m^2/g)	Pore diameter (Å)	Pore volume (cm^3/g)
Na-bentonite	51	52.31	0.063
NiP/bentonite 2 mEq/g	55	54.12	0.075
NiP/bentonite 4 mEq/g	56	54.64	0.094
NiP/bentonite 6 mEq/g	61	60.24	0.079
NiP/bentonite 8 mEq/g	67	66.68	0.113
NiP/bentonite 10 mEq/g	65	64.21	0.102

suggesting the pore blockage by the NiP species. According to Table 4, catalyst with NiP metal loading of 8 mEq/g exhibited the most optimum textural features that provided the catalytic reaction of 2-propanol conversion towards DIPE product.

Table 3 presents the total acidity of Na-bentonite and NiP/bentonite with varying NiP loadings. This approach measures the weight of the catalyst before adsorption and post-adsorption of NH_3 vapor, where the amount of NH_3 gas absorbed by the catalyst is proportional to the number of acid sites on the catalyst [63]. As shown in Table 3, Na-bentonite has a total acidity of 1.45 mmol NH_3/g, which is lower than that of the corresponding NiP/bentonite catalyst. The aluminosilicate structure of the parent bentonite is primarily responsible for its low overall acidity [6]. The total acidity of Na-bentonite gradually increased as the NiP loading increased, presumably due to the availability of Lewis acid sites from Ni and Brønsted acid sites from the phosphor species. The higher the Lewis and Brønsted sites, the higher the total acidity of the catalyst [64, 65]. The highest total acidity (4.63 mmol NH_3/g) was attained by NiP loading of 8 mEq/g. Further NiP loading (10 mEq/g) decreased the total acidity, presumably due to agglomeration, which reduced the active sites of the catalyst [66]. Wijaya et al. [67] stated that the number and distribution of active site groups on the surface that reached the maximum value caused the adsorbed base probe molecule to decrease.

Table 3 Acidity features of Na-bentonite and NiP/bentonite

Catalyst	Total acidity (mmol/g)
Na-bentonite	1.45
NiP-bentonite 2 mEq/g	2.78
NiP-bentonite 4 mEq/g	3.15
NiP-bentonite 6 mEq/g	3.57
NiP-bentonite 8 mEq/g	4.63
NiP-bentonite 10 mEq/g	3.63

Catalytic activity test

Na-bentonite and NiP/bentonite were tested for their catalytic activity in the dehydration of 2-propanol to DIPE using a fixed-bed reactor. The dehydration reaction is appreciably contingent on metal properties and metal loading [68]. Fig. 5 shows the effect of Na-bentonite and NiP/bentonite with various loadings on the DIPE product. The low acidic sites of Na-bentonite could not provide sufficient catalytic activity for DIPE production. In comparison, when the NiP species were loaded into bentonite, the DIPE product reached 64.43% at 2 mEq/g NiP loading. Prolonged NiP loading directly increased the DIPE product to 68.52%, achieved by 8 mEq/g NiP loading, presumably due to the presence of a highly acidic active site of the catalyst [36]. Meanwhile, a high NiP loading (10 mEq/g) decreased the DIPE product to 65.22%. These results were consistent with the total acidity feature acidity, which suggests that the DIPE product was mainly accelerated by the acidity of the catalyst [69]. The NiP/bentonite catalyst showed a higher DIPE product than MoP-bentonite (64.5%) [9].

The stability performance of NiP-bentonite (8 mEq/g) on the DIPE product was evaluated after three reaction cycles (Table 4). The spent catalyst was regenerated by washing and drying. The DIPE product was relatively stable within three cycles, presumably due to the strong interaction between the NiP active sites on the bentonite. However, prolonged regeneration of the catalyst probably causes the loss of active sites because of the washing process, thereby decreasing the performance of the catalyst [70].

The acidity value of the reused catalyst was further evaluated to confirm the relation between the acidity value of the catalyst with the decreased catalytic activity after three consecutive runs. The first reused catalyst decreased catalyst acidity

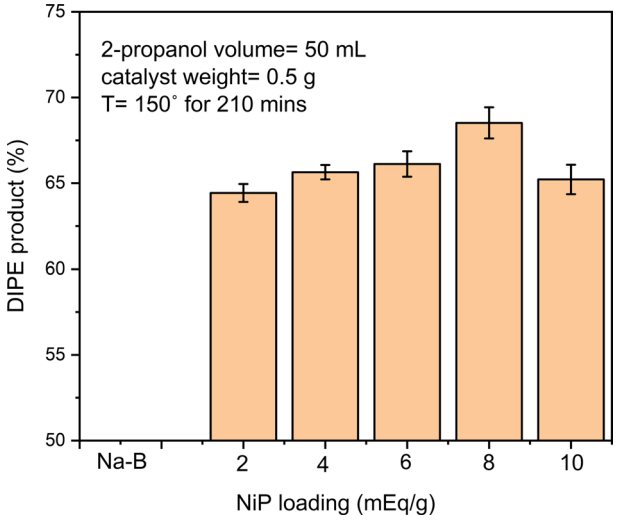

Fig. 5 DIPE production using Na-bentonite and NiP/bentonite with various NiP loading

Table 4 Reusability performance of NiP-bentonite (8 mEq/g) catalyst towards DIPE product

Cycles	DIPE product (%)
Fresh	68.50 ± 0.16
1	68.05 ± 0.11
2	67.51 ± 0.17
3	66.21 ± 0.10

from 4.63 mmol/g (fresh catalyst) to 4.59 mmol/g and tended to decrease up to 4.56 mmol/g after two consecutive runs. Moreover, the catalyst at three times reused showed a decrease in the acidity value to 4.49 mmol/g. The regeneration process could decrease catalyst acidity, implying less catalyst active site. Consequently, the catalyst performance also decreased.

Conclusion

In summary, this study evaluated the potential of nickel-phosphide-supported bentonite prepared using the wet impregnation method as an acidic catalyst for DIPE production through 2-propanol dehydration. The NiP species significantly increased the total acidity and surface area of Na-bentonite, which promoted the dehydration of 2-propanol to DIPE. XRD, FTIR, and SEM–EDX analyses revealed that the loading of NiP onto bentonite did not alter the main framework of the bentonite. A 2-propanol dehydration study showed that the NiP loading on bentonite affected the DIPE yield. The highest DIPE product, up to 68.52%, was achieved with NiP-bentonite at 8 mEq/g. This study provided a potential application of metal phosphide-supported natural bentonite for the dehydration reaction.

Acknowledgements The authors thank the Biofuel Research Group, Biofuel Research Group, Laboratory of Physical Chemistry, Faculty of Mathematics and Natural Science, Universitas Sriwijaya for providing research resources.

Data availability All experimental data in this study is available, and we can show it at any time if anyone wants further confirmation of the data.

Declarations

Conflict of interest The authors have no competing interests to declare that are relevant to the content of this article.

References

1. Chen J, Zhu L (2009) Comparative study of catalytic activity of different Fe-pillared bentonites in the presence of UV light and H_2O_2. Sep Purif Technol 67:282–288. https://doi.org/10.1016/j.seppur.2009.03.036
2. Szostak K, Banach M (2019) Sorption and photocatalytic degradation of methylene blue on bentonite-ZnO–CuO nanocomposite. J Mol Liq 286:110859. https://doi.org/10.1016/j.molliq.2019.04.136

3. Luna FMT, Cecilia JA, Saboya RMA, Barrera D, Sapag K, Rodríguez-Castellón E, Cavalcante CL (2018) Natural and modified montmorillonite clays as catalysts for synthesis of biolubricants. Materials (Basel) 11:6–9. https://doi.org/10.3390/ma11091764
4. Toor M, Jin B, Dai S, Vimonses V (2015) Activating natural bentonite as a cost-effective adsorbent for removal of Congo-red in wastewater. J Ind Eng Chem 21:653–661. https://doi.org/10.1016/j.jiec.2014.03.033
5. Hasanudin H, Asri WR, Zulaikha IS, Ayu C, Rachmat A, Riyanti F, Hadiah F, Zainul R, Maryana R (2022) Hydrocracking of crude palm oil to a biofuel using zirconium nitride and zirconium phosphide-modified bentonite. RSC Adv 12:21916–21925. https://doi.org/10.1039/d2ra03941a
6. Hasanudin H, Asri WR, Said M, Hidayati PT, Purwaningrum W, Novia N, Wijaya K (2022) Hydrocracking optimization of palm oil to bio-gasoline and bio-aviation fuels using molybdenum nitride-bentonite catalyst. RSC Adv 12:16431–16443. https://doi.org/10.1039/D2RA02438A
7. Huo J, Min X, Wang Y (2021) Zirconium-modified natural clays for phosphate removal: effect of clay minerals. Environ Res 194:110685. https://doi.org/10.1016/j.envres.2020.110685
8. Ma H-r, Hei Y-n, Hua L, Guo Y-y, Yang Y-z, Yu C-l, Qiao X-r (2016) Fabrication of zirconium-pillared montmorillonite porous ceramic as adsorbents for Cr^{3+} removal and recycling. Ceram Int 42:14903–14909. https://doi.org/10.1016/j.ceramint.2016.06.130
9. Hasanudin H, Asri WR, Tampubolon K, Riyant F, Purwaningrum W, Wijaya K (2022) Dehydration isopropyl alcohol to diisopropyl ether over molybdenum phosphide pillared bentonite. Pertanika J Sci Technol 30:1739–1754. https://doi.org/10.47836/pjst.30.2.47
10. Ngulube T, Gumbo JR, Masindi V, Maity A (2017) An update on synthetic dyes adsorption onto clay based minerals: a state-of-art review. J Environ Manage 191:35–57. https://doi.org/10.1016/j.jenvman.2016.12.031
11. Mnasri S, Hamdi N, Frini-Srasra N, Srasra E (2017) Acid–base properties of pillared interlayered clays with single and mixed Zr–Al oxide pillars prepared from Tunisian-interstratified illite–smectite. Arab J Chem 10:1175–1183. https://doi.org/10.1016/j.arabjc.2014.07.004
12. Li K, Lei J, Yuan G, Weerachanchai P, Wang JY, Zhao J, Yang Y (2017) Fe-, Ti-, Zr- and Al-pillared clays for efficient catalytic pyrolysis of mixed plastics. Chem Eng J 317:800–809. https://doi.org/10.1016/j.cej.2017.02.113
13. Bodman SD, McWhinnie WR, Begon V, Millan M, Suelves I, Lazaro MJ, Herod AA, Kandiyoti R (2003) Metal-ion pillared clays as hydrocracking catalysts (II): effect of contact time on products from coal extracts and petroleum distillation residues. Fuel 82:2309–2321. https://doi.org/10.1016/S0016-2361(03)00126-1
14. Caglar B, Cubuk O, Demir E, Coldur F, Catir M, Topcu C, Tabak A (2015) Characterization of AlFe-pillared Unye bentonite: a study of the surface acidity and catalytic property. J Mol Struct 1089:59–65. https://doi.org/10.1016/j.molstruc.2015.02.034
15. Mahadevan H, Anoop Krishnan K, Pillai RR, Sudhakaran S (2020) Stirring-ageing technique to develop zirconium-pillared bentonite clay along with its surface profiling using various spectroscopic techniques. Res Chem Intermed 46:639–660. https://doi.org/10.1007/s11164-019-03982-2
16. Agustian E, Rinaldi N, Adillina IB, Sulaswatty A, Kusuma DA (2018) Preparation of aluminium and cobalt pillared bentonite using ultrasonic treatment for vanillin catalyst. AIP Conf Proc 2024:020044. https://doi.org/10.1063/1.5064330
17. Widjaya RR, Saridewi N, Putri AA, Rinaldi N, Dwiatmoko AA (2021) Fe-Cr pillared clay as catalysts for the ethanol to gasoline conversion. IOP Conf Ser Mater Sci Eng 1011:012008. https://doi.org/10.1088/1757-899X/1011/1/012008
18. Mai NTL, Bach LG, Nhac-Vu HT, Bui QB (2020) Hierarchical star-like molybdenum phosphides nanostructures decorated graphene on 3D foam as self-supported electrocatalyst for hydrogen evolution reaction. Solid State Sci 101:106143. https://doi.org/10.1016/j.solidstatesciences.2020.106143
19. Alvarez-Galvan MC, Campos-Martin JM, Fierro JLG (2019) Transition metal phosphides for the catalytic hydrodeoxygenation of waste oils into green diesel. Catalysts 9:293. https://doi.org/10.3390/catal9030293
20. de Souza PM, Inocêncio CVM, Perez VI, Rabelo-Neto RC, Gonçalves VOO, Jacobs G, Richard F, da Silva VT, Noronha FB (2020) Hydrodeoxygenation of phenol using nickel phosphide catalysts. Study of the effect of the support. Catal Today 356:366–375. https://doi.org/10.1016/j.cattod.2019.08.028
21. Gonçalves VOO, de Souza PM, Cabioc'h T, da Silva VT, Noronha FB, Richard F (2017) Hydrodeoxygenation of m-cresol over nickel and nickel phosphide based catalysts. Influence of the nature

of the active phase and the support. Appl Catal B Environ 219:619–628. https://doi.org/10.1016/j.apcatb.2017.07.042
22. Song H, Zhang FY, Jin ZS, Wang HY, Zhu YJ, Song HL (2014) Effect of the reduction temperature on nickel phosphide catalyst structure and catalytic activity for hydrodesulfurization. Adv Mater Res 1025–1026:782–786. https://doi.org/10.4028/www.scientific.net/AMR.1025-1026.782
23. Boullosa-Eiras S, Lødeng R, Bergem H, Stöcker M, Hannevold L, Blekkan EA (2014) Catalytic hydrodeoxygenation (HDO) of phenol over supported molybdenum carbide, nitride, phosphide and oxide catalysts. Catal Today 223:44–53. https://doi.org/10.1016/j.cattod.2013.09.044
24. Akhmetzyanova U, Tišler Z, Sharkov N, Skuhrovcová L, Pelíšková L, Kikhtyanin O, Mäki-Arvela P, Opanasenko M, Peurla M, Murzin DY (2019) Molybdenum nitrides, carbides and phosphides as highly efficient catalysts for the (Hydro)deoxygenation reaction. ChemistrySelect 4:8453–8459. https://doi.org/10.1002/slct.201901634
25. Zhao HY, Li D, Bui P, Oyama ST (2011) Hydrodeoxygenation of guaiacol as model compound for pyrolysis oil on transition metal phosphide hydroprocessing catalysts. Appl Catal A Gen 391:305–310. https://doi.org/10.1016/j.apcata.2010.07.039
26. Ruangudomsakul M, Osakoo N, Wittayakun J, Keawkumay C, Butburee T, Youngjan S, Faungnawakij K, Poo-arporn Y, Kidkhunthod P, Khemthong P (2021) Hydrodeoxygenation of palm oil to green diesel products on mixed-phase nickel phosphides. Mol Catal. https://doi.org/10.1016/j.mcat.2021.111422
27. González-castaño M, Le SE, Berry C, Pastor-pérez L, Arellano-garcía H, Wang Q, Reina TR (2021) Nickel phosphide catalysts as efficient systems for CO_2 upgrading via dry reforming of methane. Catalysts 11:1–11. https://doi.org/10.3390/catal11040446
28. Yu Y, Chen Q, Li J, Rao P, Li R, Du Y, Jia C, Huang W, Luo J, Deng P, Shen Y, Tian X (2022) Progress in the development of heteroatom-doped nickel phosphates for electrocatalytic water splitting. J Colloid Interface Sci 607:1091–1102. https://doi.org/10.1016/j.jcis.2021.09.032
29. Zhao Y, Wang S, Li N, Zhang Q, Li G, Shen J (2019) Synthesis of nickel phosphide nanorods for hydrotreating reactions. Catal Commun 124:67–70. https://doi.org/10.1016/j.catcom.2019.03.006
30. Wagner JL, Jones E, Sartbaeva A, Davis SA, Torrente-Murciano L, Chuck CJ, Ting VP (2018) Zeolite Y supported nickel phosphide catalysts for the hydrodenitrogenation of quinoline as a proxy for crude bio-oils from hydrothermal liquefaction of microalgae. Dalt Trans 47:1189–1201. https://doi.org/10.1039/c7dt03318d
31. Ahmadi S, Almasi M (2020) Experimental and modeling study of diisopropyl ether and 2-alkanol; PC-SAFT model and free volume theory. J Chem Thermodyn 142:106025. https://doi.org/10.1016/j.jct.2019.106025
32. Kale AV, Krishnasamy A (2022) Investigations on load range extension of a homogeneous charge compression ignited light-duty diesel engine operated with diisopropyl ether and gasoline blends. Fuel. https://doi.org/10.1016/j.enconman.2022.115373
33. Fan X, Sun W, Liu Z, Gao Y, Yang J, Yang B, Law CK (2021) Exploring the oxidation chemistry of diisopropyl ether: jet-stirred reactor experiments and kinetic modeling. Proc Combust Inst 38:321–328. https://doi.org/10.1016/j.proci.2020.06.242
34. Armenta MA, Valdez R, Silva-Rodrigo R, Olivas A (2019) Diisopropyl ether production via 2-propanol dehydration using supported iron oxides catalysts. Fuel 236:934–941. https://doi.org/10.1016/j.fuel.2018.06.138
35. Escobar J, De Los Reyes JA, Viveros T, Valle-Orta M, Barrera MC (2015) Compensation in the isopropyl alcohol dehydration over sol–gel Al_2O_3–TiO_2 oxides: effect of calcining temperature. Fuel 149:109–117. https://doi.org/10.1016/j.fuel.2014.09.016
36. Bedia J, Ruiz-Rosas R, Rodríguez-Mirasol J, Cordero T (2010) A kinetic study of 2-propanol dehydration on carbon acid catalysts. J Catal 271:33–42. https://doi.org/10.1016/j.jcat.2010.01.023
37. Turek W, Haber J, Krowiak A (2005) Dehydration of isopropyl alcohol used as an indicator of the type and strength of catalyst acid centres. Appl Surf Sci 252:823–827. https://doi.org/10.1016/j.apsusc.2005.02.059
38. Gómez-Gutiérrez CM, Luque PA, Guerra-Rivas G, López-Sánchez JA, Armenta MA, Quintana JM, Olivas A (2015) Solvothermal synthesis of nickel-tungsten sulfides for 2-propanol dehydration. Scanning 37:165–171. https://doi.org/10.1002/sca.21194
39. Tang X, Bumueller D, Lim A, Schneider J, Heiz U, Ganteför G, Fairbrother DH, Bowen KH (2014) Catalytic dehydration of 2-propanol by size-selected (WO_3)n and (MoO_3)n metal oxide clusters. J Phys Chem C 118:29278–29286. https://doi.org/10.1021/jp505440g

40. Lin J, Jiang B, Zhan Y (2018) Effect of pre-treatment of bentonite with sodium and calcium ions on phosphate adsorption onto zirconium-modified bentonite. J Environ Manage 217:183–195. https://doi.org/10.1016/j.jenvman.2018.03.079
41. Cótica LF, Freitas VF, Santos IA, Barabach M, Anaissi FJ, Miyahara RY, Sarvezuk PWC (2011) Cobalt-modified Brazilian bentonites: preparation, characterisation, and thermal stability. Appl Clay Sci 51:187–191. https://doi.org/10.1016/j.clay.2010.10.033
42. Zaki T, Mukhtarova GS, Al-Sabagh AM, Soliman FS, Betiha MA, Mahmoud T, Abd El-Raouf M, Afandiyeva NK, Alizade A, Hasanova AB, Abbasov VM (2018) Slurry-phase catalytic hydrocracking of mazut (heavy residual fuel oil) using Ni-bentonite. Pet Sci Technol 36:1559–1567. https://doi.org/10.1080/10916466.2018.1490762
43. Cao Y, Zhou G, Zhou R, Wang C, Chi B, Wang Y, Hua C, Qiu J, Jin Y, Wu S (2020) Green synthesis of reusable multifunctional γ-Fe_2O_3/bentonite modified by doped TiO_2 hollow spherical nanocomposite for removal of BPA. Sci Total Environ 708:134669. https://doi.org/10.1016/j.scitotenv.2019.134669
44. Sadek SA, Solyman SM, Abdel-Samad HS, Hassan SA (2010) Catalytic behavior of cobalt (II) phthalocyanine immobilized on bentonite clay in bulk polymerization of methyl methacrylate. Int J Polym Mater Polym Biomater 59:353–369. https://doi.org/10.1080/00914030903478925
45. Wu X, Li J, Li Y, Wen Z (2021) NiFeP-MoO_2 hybrid nanorods on nickel foam as high-activity and high-stability electrode for overall water splitting. Chem Eng J 409:128161. https://doi.org/10.1016/j.cej.2020.128161
46. El-Nagar DA, Sary DH (2021) Synthesis and characterization of nano bentonite and its effect on some properties of sandy soils. Soil Tillage Res 208:104872. https://doi.org/10.1016/j.still.2020.104872
47. Li S-w, Pan J, Zhu D-q, Guo Z-q, Xu J-w, Chou J-l (2020) Synthesis, characterization and properties of organically compounded bentonite by molecular intercalation process. J Iron Steel Res Int 27:1127–1136. https://doi.org/10.1007/s42243-020-00385-1
48. Pajarito BB, Castañeda KC, Jeresano SDM, Repoquit DAN (2018) Reduction of offensive odor from natural rubber using zinc-modified bentonite. Adv Mater Sci Eng 2018:9102825. https://doi.org/10.1155/2018/9102825
49. Ravari MH, Sarrafi A, Tahmooresi M (2020) Synthesizing and characterizing the mixed Al, Cu-pillared and copper doped Al-pillared bentonite for electrocatalytic reduction of C_O2. South African J Chem Eng 31:1–6. https://doi.org/10.1016/j.sajce.2019.10.001
50. Zong P, Shao M, Xu X, Xu M, Yan N, Wang S, Yang Y, Chen J, Qiu Z (2022) Prediction and optimization of removal performance for europium onto phosphate decorated zirconium-based metal–organic framework nanocomposites: Structure-activity relationship and mechanism evaluation. J Mol Liq 360:119565. https://doi.org/10.1016/j.molliq.2022.119565
51. Bhatt R, Ageetha V, Rathod SB, Padmaja P (2019) Self-assembled chitosan-zirconium phosphate nanostructures for adsorption of chromium and degradation of dyes. Carbohydr Polym 208:441–450. https://doi.org/10.1016/j.carbpol.2018.12.077
52. Zhao Y, Yan S, He Y, Li Z, Li C, Li H (2022) Synthesis of ultrathin α-zirconium phosphate functionalized with polypyrrole for reinforcing the anticorrosive property of waterborne epoxy coating. Colloids Surfaces A Physicochem Eng Asp. https://doi.org/10.1016/j.colsurfa.2021.128052
53. Wang J, Wei Y, Wang J, Zhang X, Wang Y, Li N (2022) Simultaneous immobilization of radionuclides Sr and Cs by sodium zirconium phosphate type ceramics and its chemical durability. Ceram Int 48:12772–12778. https://doi.org/10.1016/j.ceramint.2022.01.147
54. Babu AT, Antony R (2019) Clay semiconductor hetero-system of SnO_2/bentonite nanocomposites for catalytic degradation of toxic organic wastes. Appl Clay Sci 183:105312. https://doi.org/10.1016/j.clay.2019.105312
55. de Nazaré de Oliveira A, de Lima MAB, de Oliveira Pires LH, da Silva MR, da Luz PTS, Angélica RS, da Rocha Filho GN, da Costa CEF, Luque R, do Nascimento LAS (2019) Bentonites modified with phosphomolybdic heteropolyacid (HPMo) for biowaste to biofuel production. Materials 12:1431. https://doi.org/10.3390/ma12091431
56. Kadeche A, Ramdani A, Adjdir M, Guendouzi A, Taleb S, Kaid M, Deratani A (2020) Preparation, characterization and application of Fe-pillared bentonite to the removal of Coomassie blue dye from aqueous solutions. Res Chem Intermed 46:4985–5008. https://doi.org/10.1007/s11164-020-04236-2
57. Abdou MI, Al-sabagh AM, Dardir MM (2013) Evaluation of Egyptian bentonite and nano-bentonite as drilling mud. Egypt J Pet 22:53–59. https://doi.org/10.1016/j.ejpe.2012.07.002

58. Wang YY, Chen BH (2016) High-silica zeolite beta as a heterogeneous catalyst in transesterification of triolein for biodiesel production. Catal Today 278:335–343. https://doi.org/10.1016/j.cattod.2016.03.012
59. Cortés JC, Muñoz M, Macías L, Molina R, Moreno S (2017) Incorporation of Ni and Mo on delaminated clay by auto-combustion and impregnation for obtaining decane hydroconversion catalysts. Catal Today 296:205–213. https://doi.org/10.1016/j.cattod.2017.08.028
60. Moma J, Baloyi J, Ntho T (2018) Synthesis and characterization of an efficient and stable Al/Fe pillared clay catalyst for the catalytic wet air oxidation of phenol. RSC Adv 8:30115–30124. https://doi.org/10.1039/c8ra05825c
61. Bertella F, Pergher SBC (2017) Reuse of pillaring agent in sequential bentonite pillaring processes. Materials. https://doi.org/10.3390/ma10070705
62. Mirzan M, Wijaya K, Falah II, Trisunaryanti W (2019) Synthesis and characterization of Ni/ZrO_2-bentonite. Asian J Chem 31:229–234
63. Wijaya K, Kurniawan MA, Saputri WD, Trisunaryanti W, Mirzan M, Hariani PL, Tikoalu AD (2021) Synthesis of nickel catalyst supported on ZrO_2/SO_4 pillared bentonite and its application for conversion of coconut oil into gasoline via hydrocracking process. J Environ Chem Eng 9:105399. https://doi.org/10.1016/j.jece.2021.105399
64. Hauli L, Wijaya K, Syoufian A (2020) Fuel production from LDPE-based plastic waste over chromium supported on sulfated zirconia. Indones J Chem 20:422–429. https://doi.org/10.22146/ijc.45694
65. Utami M, Safitri R, Fajar Pradipta M, Wijaya K, Woong Chang S, Ravindran B, Ovi D, Rajabathar JR, Poudineh N, Moonsamy Gengan R (2022) Enhanced catalytic conversion of palm oil into biofuels by Cr-incorporated sulphated zirconia. Mater Lett 309:131472. https://doi.org/10.1016/j.matlet.2021.131472
66. Wijaya K, Nadia A, Dinana A, Pratiwi AF, Tikoalu AD, Wibowo AC (2021) Catalytic hydrocracking of fresh and waste frying oil over Ni-and Mo-based catalysts supported on sulfated silica for biogasoline production. Catalysts 11:1150. https://doi.org/10.3390/catal11101150
67. Wijaya K, Malau LLM, Utami M, Mulijani S, Patah A, Wibowo AC, Chandrasekaran M, Rajabathar JR, Al-Lohedan HA (2021) Synthesis, characterizations and catalysis of sulfated silica and nickel modified silica catalysts for diethyl ether (DEE) production from ethanol towards renewable energy applications. Catalysts 11:1511. https://doi.org/10.3390/catal11121511
68. Said AEAA, El-Aal MA (2018) Effect of different metal sulfate precursors on structural and catalytic performance of zirconia in dehydration of methanol to dimethyl ether. J Fuel Chem Technol 46:67–74. https://doi.org/10.1016/s1872-5813(18)30004-5
69. Ni W, Li D, Zhao X, Ma W, Kong K, Gu Q, Chen M, Hou Z (2019) Catalytic dehydration of sorbitol and fructose by acid-modified zirconium phosphate. Catal Today 319:66–75. https://doi.org/10.1016/j.cattod.2018.03.034
70. Hasanudin H, Asri WR, Andini L, Riyanti F, Mara A, Hadiah F, Fanani Z (2022) Enhanced isopropyl alcohol conversion over acidic nickel phosphate-supported zeolite catalysts. ACS Omega 7:38923–38932. https://doi.org/10.1021/acsomega.2c04647